CHARACTERIZATION AND ANTIOXIDANT ACTIVITY OF POLYACRYLIC ACID MODIFIED WITH SEVERAL ALDEHYDES USING BENZIDINE AS A SPACER

A.R. Kadhim, S.A. Aowda, M.M. Kareem*

Department of Chemistry, College of Science, University of Babylon, Babylon, 51002 Iraq
**email: Sci.mohanad.mousa@uobabylon.edu.iq*

Received 24.09.2025
Accepted 04.12.2025

Abstract: Polyacrylic acid has been utilized to react with a variety of substances to create novel compounds with biological activity because it is a recognized safe material to work with. In this work, the AB chemical was created by reacting polyacrylic acid with benzidine. It was then combined with a class of cyclic aldehydes to create novel Schiff-base compounds with biological advantages. FT-IR and ^{1}H-NMR spectroscopy were used to characterize them. Their melting point, solubility in various solvents, viscosity, and biological activity against gram-positive and gram-negative bacteria were all measured. Each sample's antioxidant activity was assessed and compared to ascorbic acid.
Key words: polyacrylic acid, biological activity, Schiff-base compounds, anti-oxidant activity.

Introduction

Hydrogels are often made of hydrophilic organic networks that have a lot of water incorporated into them. Because of this, they have soft and elastic qualities that fit in with human physiology. In addition to loading a wide range of medications into their structures, many hydrogels may also significantly shield them from physiological circumstances, especially those of the stomach, where the pH is low and the concentration of enzymes is high—conditions that make many medications unstable. Beyond this protective feature, hydrogels could be engineered to deliver a targeted drug release by selectively releasing medications under physiological conditions at the illness site in the body. As a result, hydrogels have been widely used in research on drug delivery [1-4].

High molecular weight synthetic (manufactured) polyacrylic acid (PAA), originally known as poly 1-carboxyethylene, is a polymer derived from acrylic acid monomers. PAA has high hydrophilicity and is responsive to pH because part or all of the carboxyl groups along its backbone can ionize depending on the acidity of their environment in aqueous media. This leads to significant changes in the polymer chain's conformation: osmotic swelling pressure increases with increasing degree of ionization, and so too does overall viscosity. PAA molecules are large and polydisperse. Solvability, charge density, and hydrogen bonding capability, all phenomena being influenced by molecular weight in homogeneous systems, are not exceptions to this rule. Capping the chain will make PAA a new kind of inhomogeneous system, and a responsive way of controlling molecular weight will synthesize composite materials, which in their turn may bring about even more drastic transformation in polymers' properties. Water-soluble, non-toxic, and recyclable, it is a biocompatible superabsorbent polymer [5, 6].

Superabsorbent polymers (SAP) are net-organized, hydrophilic polymers such as amines, carboxylic acids, and hydroxyls. In contrast to conventional water-absorbing polymers, superabsorbents have the ability to absorb large amounts of water and remove it even when under pressure. Superabsorbents' remarkable properties make them widely used in sewage treatment, biomedical and everyday physiological products, farming, healthcare, and isolation techniques [7, 8].

Schiff bases are made from carbonyl and amino compounds that coordinate with metal ions through the nitrogen atom of an azomethine [9]. It has been observed that Azomethine (C=N) exhibits exceptional biological and antibacterial properties [10, 11].

Worldwide research is being done on the synthesis, characterization, and structure-activity relationship (SAR) of Schiff bases. Numerous investigations demonstrated the significant chemical and biological significance of a single pair of electrons in the sp^2 hybridized orbital of the nitrogen

atom of the azomethine group [12]. By creating a hydrogen link between the active centers of cell constituents and the sp2 hybridized nitrogen atom of the azomethine group, they disrupt regular cell functions [13, 14].

Schiff bases may also be used as corrosion inhibitors [16], dyes, pigments, catalysts, polymer stabilizers [15], and organic synthesis intermediates. Schiff base metal complexes are more effective than free organic ligands, according to several studies [17]. According to numerous studies, adding transition metals to Schiff bases boosts their biological activity [18].

Schiff bases are essential to the discovery and development of new molecules with strong biological activity in coordination chemistry. The usefulness of Schiff bases, which are the intermediates in organic processes, is being investigated further. Researchers have focused on Schiff bases and their derivatives to investigate different procedures for the creation of new environmentally friendly technologies [19].

Researchers are currently paying attention to Schiff bases in the medical field because of their chemotherapeutic uses. They are known to display a wide range of powerful behaviors. Nitrogen-containing heterocyclic compounds exhibit a variety of biological characteristics. As an important class of heterocyclic compounds, Schiff bases exhibit antioxidant, anticonvulsant, depressive, anti-inflammatory, analgesic, antibacterial, antimalarial, and anticancer properties [20, 21].

These compounds play an important role in the manufacture of numerous physiologically and medicinally active compounds. Schiff bases and their derivatives are also regarded as crucial intermediates in the synthesis of heterocyclic compounds that contain nitrogen. The R-CH=N-Ar formula is frequently used to express them [22, 23].

The structure of naturally occurring compounds frequently contains Schiff bases. They play a significant part in pharmaceutical research and synthesis. Fig. 1 shows the chemical structures of a few Schiff bases that are pharmacologically active.

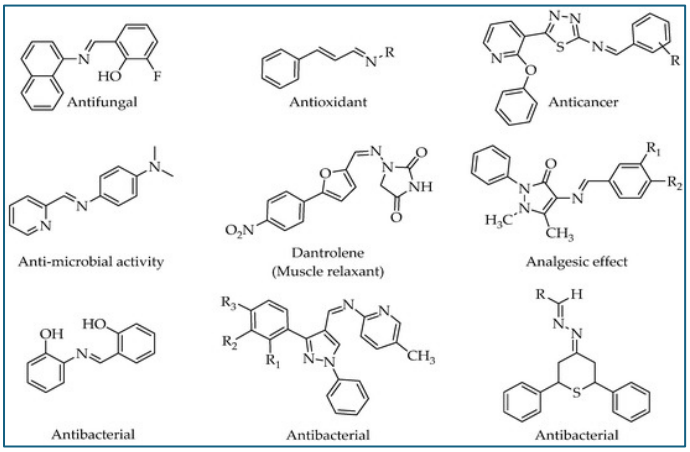

Fig. 1. Chemical structures of some pharmacologically active Schiff bases [24]

Experimental part

Materials used. Fluka, Sigma-Aldrich, CDH, and Riedel-de Haen Company provided analytical-grade solvents and reagents for the analysis, including benzaldehyde, cinnamon aldehyde, salicylaldehyde, 4-nitrobenzaldehyde, 4-chlorobenzaldehyde, and 4-bromobenzaldehyde. A Bruker Tensor II Fourier Transform Infrared Spectrometer was used to record Fourier Transform Infrared (FTIR) spectra. A Bruker Tensor II Fourier Transform Infrared Spectrometer Promoter ATR-FTIR was used to record the ATR FTIR spectra in the 400–4000 cm^{-1} range. The PG CECIL CE7200 double-beam spectrophotometer was used to assess UV absorption. Using TMS as the reference standard, 1H NMR spectra in dimethyl sulfoxide [DMSO] were generated using a Varian INOVA 500 MHz NMR spectrometer. Chemical changes were described in parts per million (ppm).

Modification of polyacrylic acid with benzidine (AB). After dissolving 0.5 g (0.00025 mole) of polyacrylic acid in 10 ml of DMF, 1.29 g (0.007 mole) of benzidine, and 6 drops (0.082 mol) from

$SOCl_2$, the mixture was vigorously stirred for one hour at room temperature. A precipitate was produced, and the solvent was removed, cleaned with ether, and allowed to dry at room temperature [25, 26].

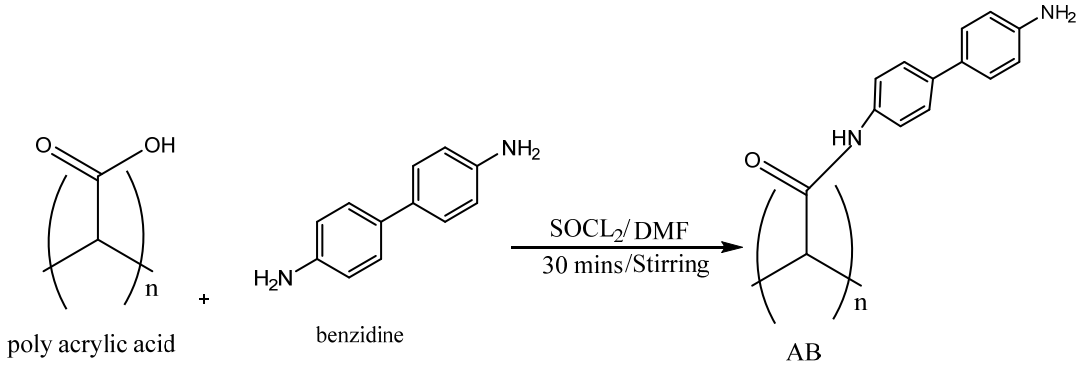

Equation 1. Synthesis of compound AB

Synthesis of C1-C6 compounds. Refluxing a mixture has produced the Schiff base compounds of 2.1 mmole of aldehydes [(10 drop) benzoaldehyde, (10 drop) cinnamon aldehyde, (10 drop) salicyl aldehyde, (0.32 gm)] 4-nitrobenzaldehyde, 0.3 gm of 4-chlorobenzaldehyde, and 0.4 gm of 4-bromobenzaldehyde, and 0.075 mmole (0.5 gm) of AB in 15 ml of ethanol were refluxed for almost three hours. The resulting Schiff base was allowed to cool to room temperature and collected by filtration; then it was recrystallized in ethanol and dried at room temperature [27].

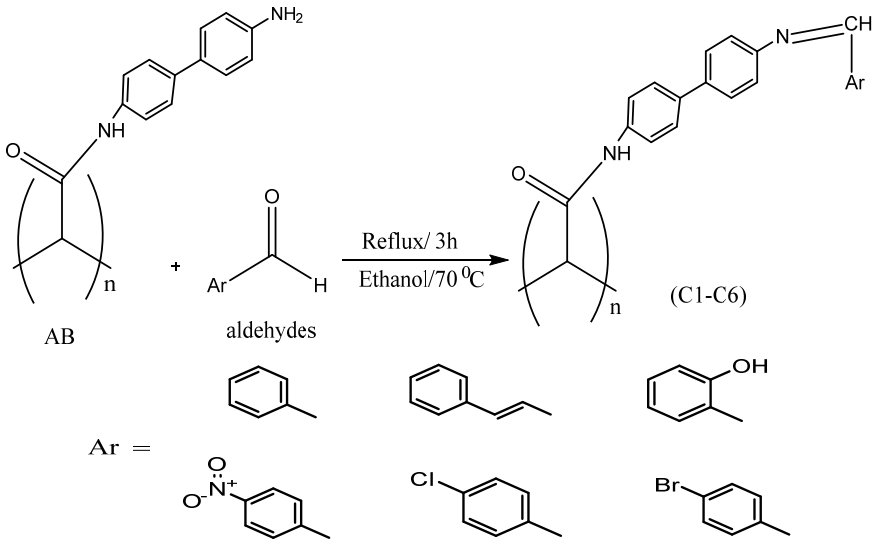

Scheme 1. General scheme for Synthesis of compounds (C1-C6)

Table 1 describes the physical properties of the synthesized compounds after conjugation with aldehydes. In terms of color and melting points of the resulting compounds.

Table1. Physical properties of polymers C1-C6.

Compound	**Color**	**m.p ºC**
C1	Light Yellow	300^0C >
C2	Dark Yellow	300 ^{0}C>
C3	Light Brown	205-208 ^{0}C
C4	Red	297-300 ^{0}C
C5	Light Brown	245-248 ^{0}C
C6	Light Yellow	290-293 ^{0}C

Results and discussion

Scheme 2 captures a classic acid-catalyzed formation of a carboxamide. The carboxylic acid (blue) first becomes protonated, making its carbonyl more eager for attack. The amine (red) then strikes the activated carbonyl, forming a fleeting tetrahedral intermediate that shuffles protons. Depending on where the proton sits, the structure flips between neutral and charged forms, but all roads lead to the same dehydrating step: the intermediate loses water, restoring the carbonyl and yielding the amide. The acid helps both in activating the carbonyl and in escorting protons to the right places, while the amine provides the nucleophilic punch.

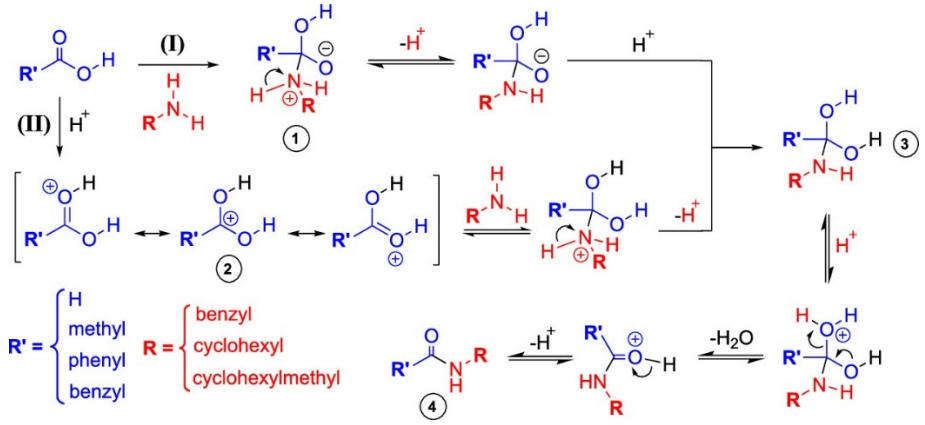

Scheme 2. Mechanism of the synthesis of compound AB according to the reference [28]

The Scheme 3 shows how an aldehyde and a primary amine join forces to form a Schiff base. The amine first attacks the aldehyde's carbonyl carbon, giving a charged, temporary carbinolamine. Protons shuffle around until the molecule is poised to lose water. Dehydration tightens the structure into an iminium ion, and one final proton loss locks in the double bond between carbon and nitrogen. What begins as a simple carbonyl ends as a C=N imine, a neat little transformation powered by nucleophilic attack, proton choreography, and dehydration.

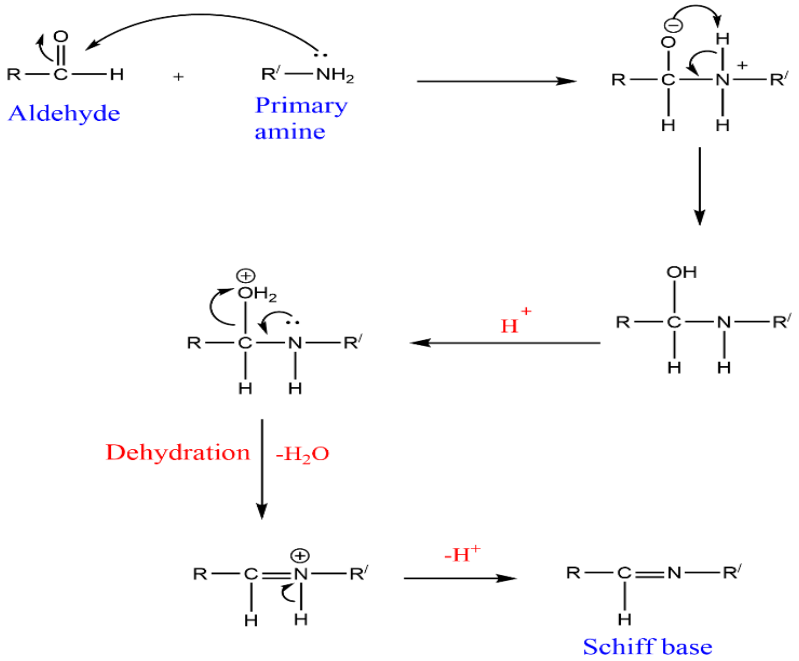

Scheme 3. Mechanism of the synthesis of compounds C1-C6

New Schiff-base polymers were prepared in good yield by reacting polyacrylic acid with benzidine and a series of aldehydes, including benzaldehyde, cinnamaldehyde, salicylaldehyde, and the substituted 4-nitro, 4-chloro, and 4-bromobenzaldehydes. The resulting materials were characterized by FTIR and ^{1}H NMR spectroscopy, while their viscosities were measured to estimate

molecular weights, and their solubility was evaluated across various solvents. Antibacterial activity was assessed against both a Gram-negative strain *(E. coli)* and a Gram-positive strain *(S. aureus)*, and the antioxidant performance of the compounds was determined in comparison with ascorbic acid [14, 20].

For compound C1, the ^{1}H NMR spectrum displays characteristic signals at 1.4 ppm assigned to the CH–CH$_2$ protons and 2.2 ppm corresponding to the O=C–CH group. The aromatic protons (Ar–CH=CH) resonate in the range of 6.5–8.0 ppm. A distinct signal at 8.7 ppm is attributed to the azomethine proton (–N=CH), while the resonance at 5.3 ppm corresponds to the amide proton (–CONH–).

The FTIR spectrum further confirms the proposed structure. A broad absorption band observed at 3000–3500 cm^{-1} is assigned to N–H stretching vibrations. The appearance of a new amide carbonyl band at 1620.21 cm^{-1} and a new azomethine (C=N) stretching band at 1666.50 cm^{-1} indicates the successful formation of amide and Schiff base functionalities. Moreover, the disappearance of the characteristic absorption bands corresponding to the carboxylic –OH group of poly(acrylic acid) and the aldehyde C=O group confirms the completion of the condensation reaction.

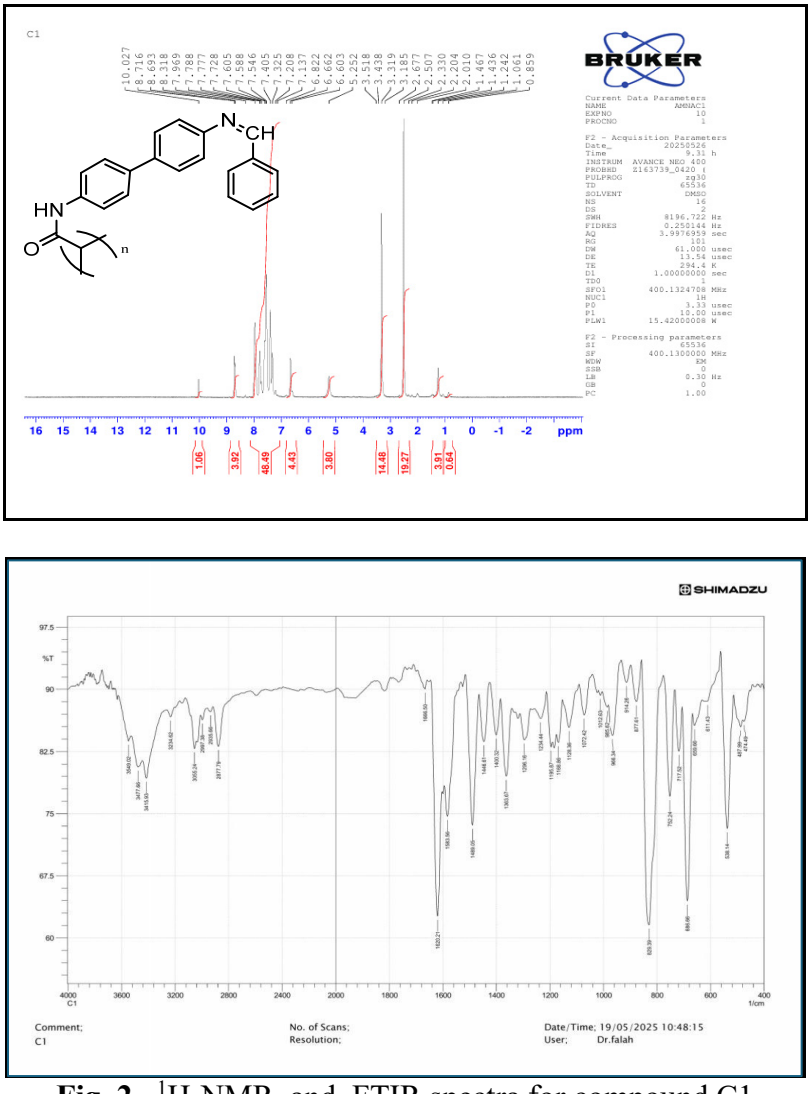

Fig. 2. ^{1}H-NMR and FTIR spectra for compound C1

Additional absorption bands are observed in the region of 1400.32–1583.56 cm^{-1} for aromatic C=C stretching vibrations, at approximately 3300 cm^{-1} for aliphatic –CH stretching, 3000–3100 cm^{-1} for aliphatic –CH$_2$ groups, and 3050–3150 cm^{-1} for aromatic –CH stretching vibrations (Fig. 2).

For compound C2, the ^{1}H NMR spectrum shows CH-CH$_2$ at 1.3 ppm; O=C-CH at 2.2 ppm; (Ar.) CH=CH at 7.1-7.8 ppm; N=C-H at 8.5 ppm; O=C-NH at 5.3 ppm; (Ar.) CH=C-CH at 2.3 ppm; (Alph.) C=C-H at 6.5 ppm. The FTIR spectrum shows NH 3000-3500 cm^{-1}, a new C=O amide group

at 1622.13 cm^{-1}, a new C=N Schiff base group at 1666.50 cm^{-1}, and the disappearance of the –OH carboxyl group of polyacrylic acid and C=O aldehyde; CH=CH (Ar.) 1400.32-1579.70 cm^{-1}; CH=CH (Alph) 1600-1680 cm^{-1}; -CH (Alph.) 3300 cm^{-1}; -CH_2 (Alph.) 3000-3100 cm^{-1}; and -CH (Ar.) 3050-3150 cm^{-1} (Fig. 3).

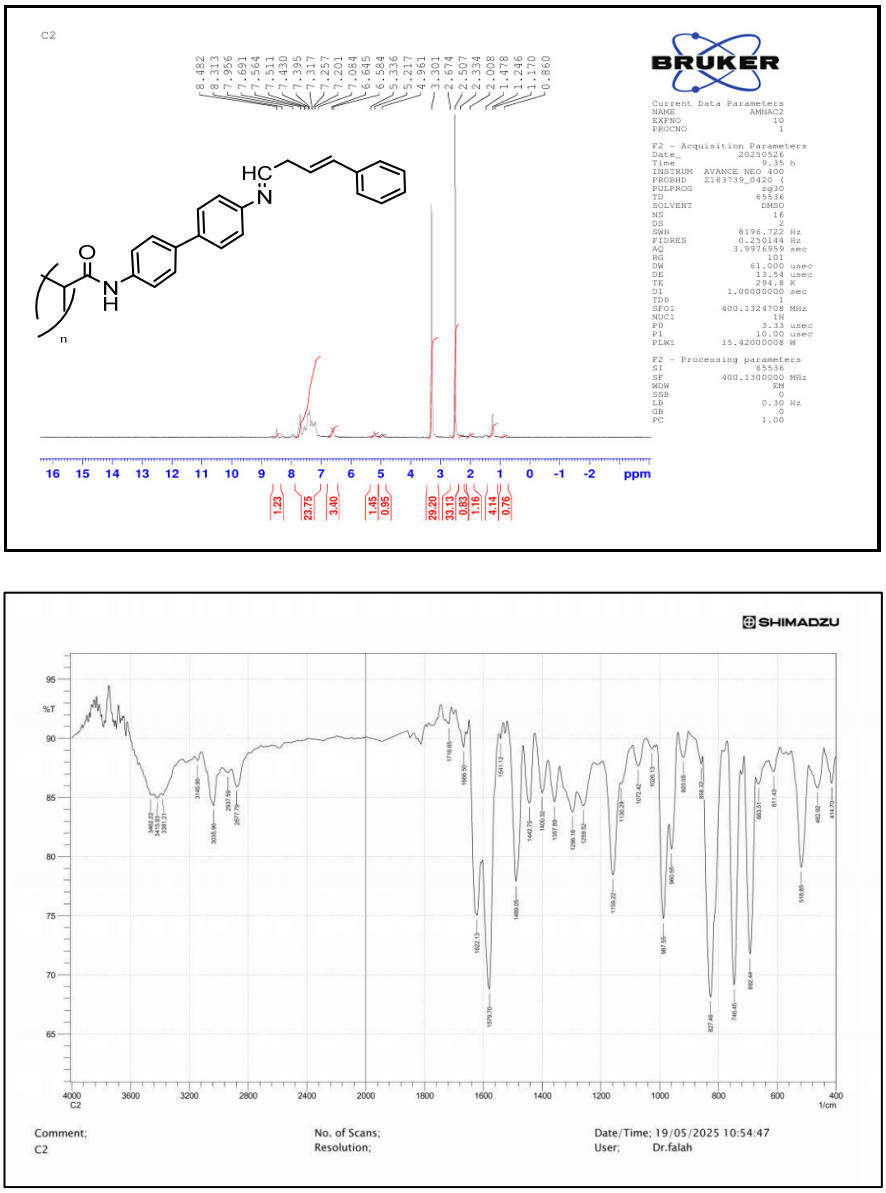

Fig. 3. [1]HNMR and FTIR spectra for compound C2

For compound C3 the [1]HNMR spectrum shows: CH-CH_2 1.2-1.4 ppm; O=C-CH 2.1 ppm; (Ar.) CH=CH 7.2-7.9 ppm; N=C-H 8.4 ppm; O=C-NH 5.9 ppm; (Ar.)-OH 6.7 ppm. FTIR spectrum shows: NH- 3000-3500 cm^{-1}; new C=O amide group at 1614.42$cm^{-1}$and new C=N Schiff base group at 1683.86 cm^{-1} and disappearing of –OH carboxyl group of polyacrylic acid and C=O aldehyde ; CH=CH (Ar.) 1408.04-1568.13 cm^{-1};C-OH 3417.86 cm^{-1},-CH (Alph.) 3300 cm^{-1} ;-CH_2 (Alph.) 3000-3100 cm^{-1} ; -CH (Ar.) 3050-3150 cm^{-1} (Fig. 4).

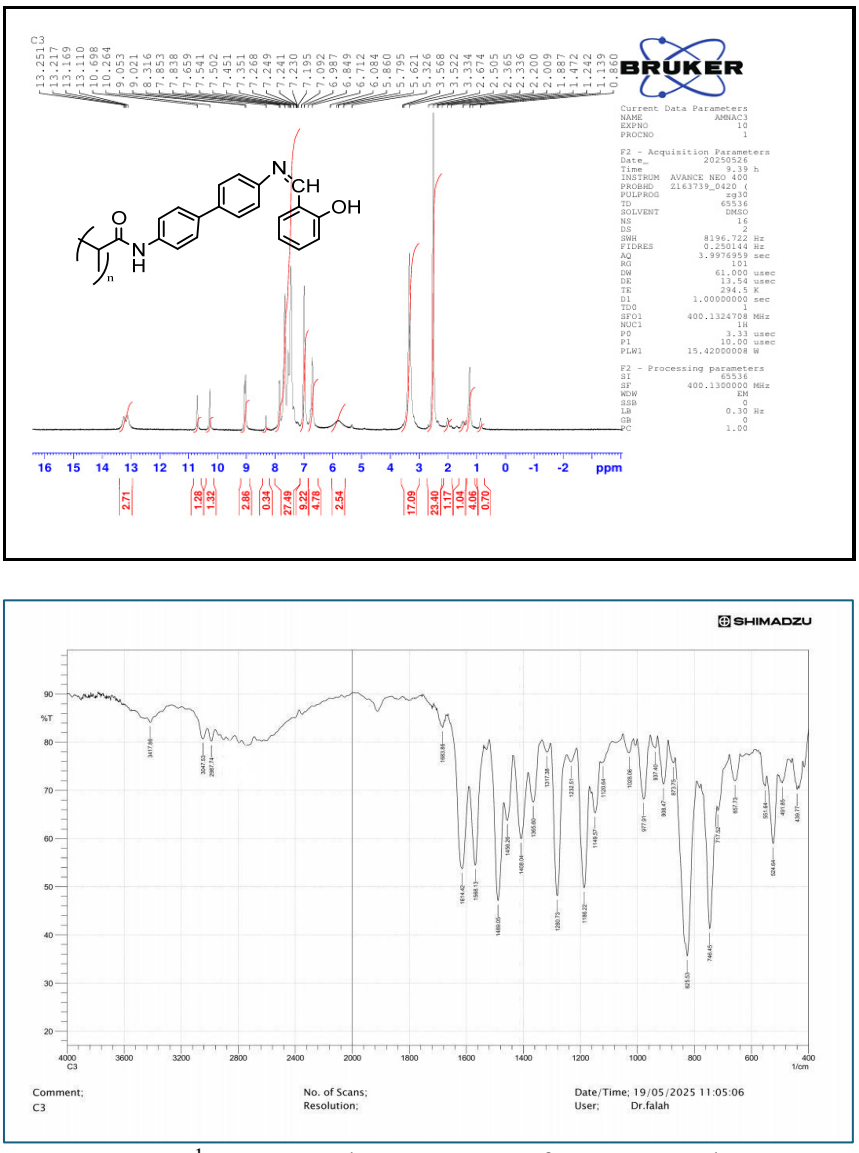

Fig. 4. [1]HNMR and FTIR spectra for compound C3

For compound C4**,** the [1]H NMR spectrum exhibits the following characteristic signals: a resonance at 1.2 ppm assigned to the CH–CH_2 protons; a signal at 2.2 ppm corresponding to the O=C–CH group; aromatic protons (Ar–CH=CH) appearing in the range of 6.8–8.0 ppm; a singlet at 8.5 ppm attributed to the azomethine proton (N=CH); and a signal at 5.4 ppm assigned to the amide proton (O=C–NH).

The FTIR spectrum confirms the formation of the target structure. A broad absorption band at 3000–3500 cm^{-1} corresponds to N–H stretching vibrations. The appearance of a new amide carbonyl band at 1600.92 cm^{-1} and a new azomethine (C=N) band at **1624.06 cm^{-1}** indicates successful formation of both amide and Schiff base functionalities. Notably, the characteristic absorption bands of the carboxylic –OH group of poly(acrylic acid) and the aldehyde C=O group disappear, further confirming the reaction progress.

Additional absorption bands are observed at 1409.96–1575.84 cm^{-1} for aromatic C=C stretching vibrations, 1344.38 cm^{-1} for N=O stretching, approximately 3300 cm^{-1} for aliphatic –CH stretching, 3000–3100 cm^{-1} for aliphatic –CH_2 groups, and 3050–3150 cm^{-1} for aromatic –CH stretching vibrations (Fig. 5).

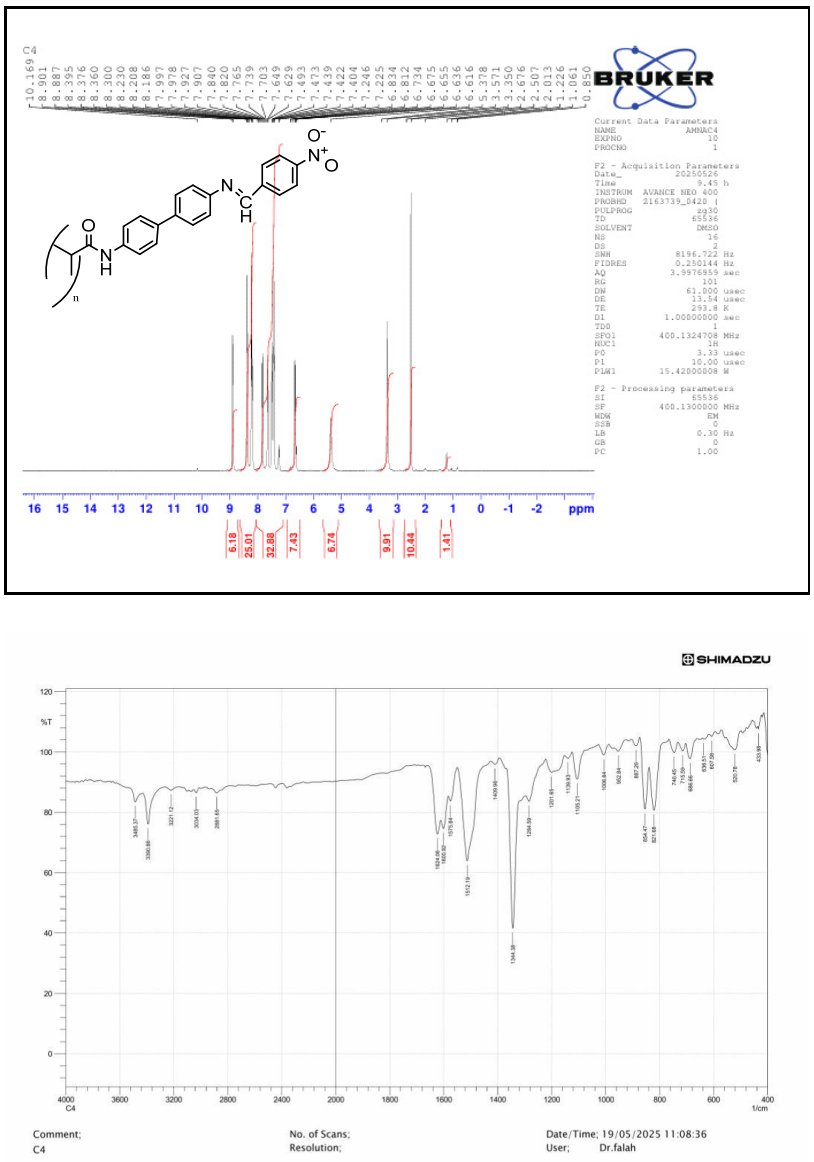

Fig. 5. [1]HNMR and FTIR spectra for compound C4

For Compound C5 the [1]HNMR spectrum shows: CH-CH_2 1.6 ppm; O=C-CH 2.1 ppm; (Ar.) CH=CH 6.5-7.9 ppm; N=C-H 8.7 ppm; O=C-NH 5.5 ppm. FTIR spectrum shows: NH- 3000-3500 cm^{-1}; new C=O amide group at 1622.13 $cm^{-1}$and new C=N shiff base group at 1670.35 cm^{-1} and disappearing of –OH carboxyl group of polyacrylic acid and C=O aldehyde; CH=CH (Ar.) 1402.25-1587.42 cm^{-1}; C-Cl 634.58-719.45; -CH (Alph.) 3300 cm^{-1}; -CH_2 (Alph.) 3000-3100 cm^{-1}; -CH (Ar.) 3050-3150 cm^{-1} (Fig.6).

For compound **C6**, the **^{1}H NMR spectrum** shows characteristic signals at **1.4 ppm**, assigned to the CH–CH_2 protons, and **2.0 ppm**, corresponding to the O=C–CH group. The aromatic protons (Ar–CH=CH) resonate in the region of **6.5–8.0 ppm**. A distinct signal at **8.6 ppm** is attributed to the azomethine proton (–N=CH), while the resonance at **5.4 ppm** corresponds to the amide proton (–CONH–).

The **FTIR spectrum** further confirms the formation of the target structure. A broad absorption band in the range of **3000–3500 cm^{-1}** is assigned to N–H stretching vibrations. The appearance of a new amide carbonyl band at **1620.21 cm^{-1}** and a new azomethine (C=N) stretching band at **1668.43 cm^{-1}** indicates successful formation of the amide and Schiff base functionalities. The disappearance of the characteristic absorption bands corresponding to the carboxylic –OH group of poly(acrylic acid) and the aldehyde C=O group further confirms completion of the condensation reaction.

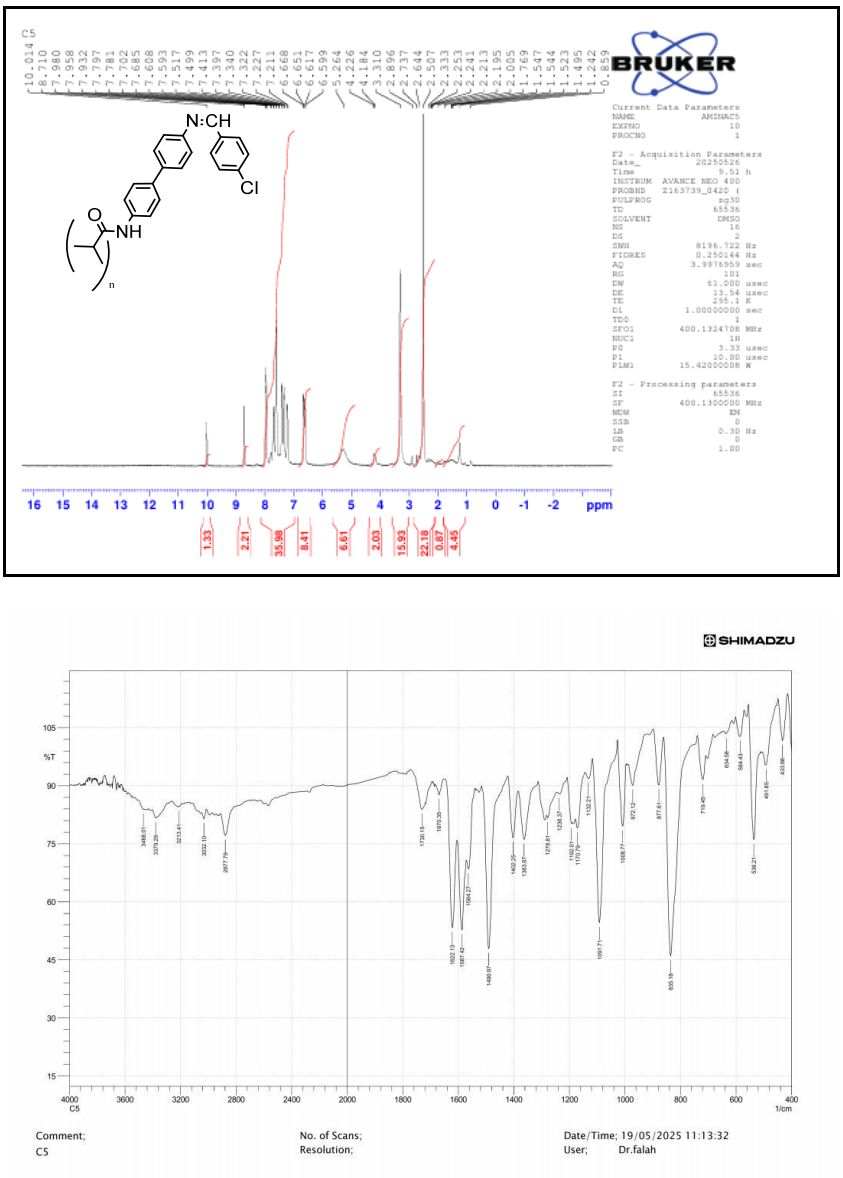

Fig. 6. [1]HNMR and FTIR spectra for compound C5

Additional absorption bands observed in the region of **1402.25–1585.49 cm⁻¹** correspond to aromatic C=C stretching vibrations. The band at **536.21 cm⁻¹** is assigned to C–Br stretching vibrations. Further bands include aliphatic –CH stretching at approximately **3300 cm⁻¹**, aliphatic –CH_2 stretching at **3000–3100 cm⁻¹**, and aromatic –CH stretching vibrations at **3050–3150 cm⁻¹** (Fig. 7).

The Schiff base derivatives synthesized via the reaction of poly(acrylic acid) with benzidine and various aldehydes exhibit limited solubility in common organic solvents. This reduced solubility can be primarily attributed to the high molecular weight and complex macromolecular architecture of the resulting polymeric structures. Moreover, strong intermolecular interactions, including extensive hydrogen bonding, π–π stacking between aromatic moieties, and possible interchain cross-linking, significantly hinder solvent diffusion into the polymer matrix.

The coexistence of polar functional groups (amide, imine, and residual carboxyl groups) and hydrophobic aromatic segments further complicates solvent compatibility, often leading to only partial swelling rather than complete dissolution. Consequently, effective solubilization typically requires highly polar aprotic solvents such as dimethyl sulfoxide (DMSO) or dimethylformamide (DMF), elevated temperatures, or appropriate solvent mixtures to disrupt intermolecular interactions and enhance polymer–solvent interactions [28].

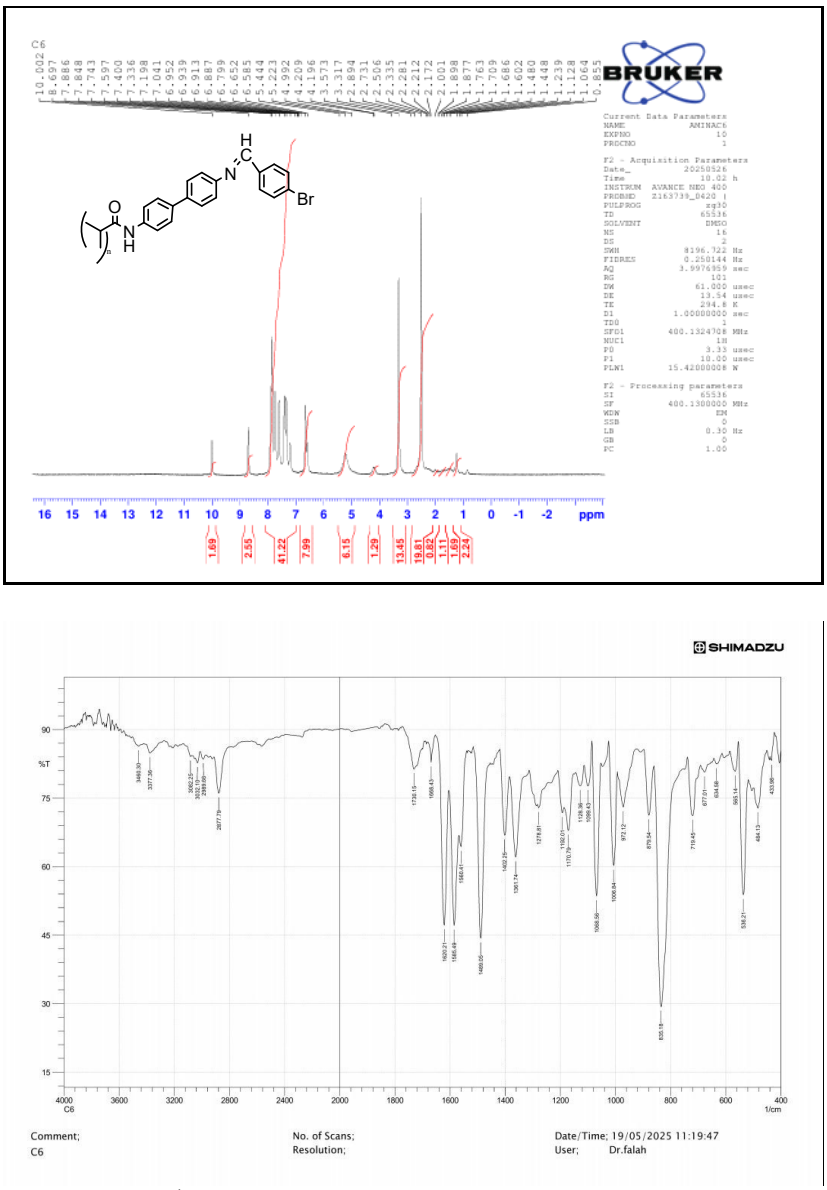

Fig. 7. [1]HNMR and FTIR spectra for compound C6.

Table 2. Solubility of the polymers C1-C6.

Compounds / Solvents	H_2O	EtOH	MeOH	DMF	DMSO	DCM	CH_3Cl	ether	Diethyl ether	Acetone
C1	-	P.	P.	+	+	+	+	P.	P.	P.
C2	-	P.	P.	+	+	P.	+	P.	P.	P.
C3	-	P.	P.	+	+	P.	+	P.	P.	P.
C4	P.	P.	P.	+	+	+	+	P.	+	+
C5	-	P.	P.	+	+	+	+	P.	P.	P.
C6	P.	P.	P.	+	+	P.	+	P.	P.	P.

Intrinsic viscosity measurements were performed using a viscometer, and the viscosity–average molecular weight was determined according to the Mark–Houwink equation:

$$[\eta]=KM^{a}$$

This empirical relationship describes the dependence of a polymer's intrinsic viscosity [η] on its molecular weight. In this equation, [η] represents the intrinsic viscosity, *K* and *a* are constants characteristic of a given polymer–solvent system at a specific temperature, and *M* corresponds to the viscosity–average molecular weight. The values of *K* and *a* depend on factors such as solvent type, polymer structure, and measurement temperature.

Among the synthesized compounds, **C5** exhibited the highest intrinsic viscosity (Tables 3–8), indicating a comparatively higher viscosity–average molecular weight. This behavior may be attributed to the structural characteristics of the aldehyde moiety incorporated into C5, which likely enhances intermolecular interactions and chain rigidity, thereby increasing hydrodynamic volume in solution.

According to the Mark–Houwink relationship, intrinsic viscosity increases with molecular weight, confirming the direct correlation between polymer chain length and solution viscosity.

Table 3. Data of C1 used to determine the intrinsic viscosity

C1 compound concentration, mg/ml	Time flow t/s	ηsp=(η/η$_o$=t/t$_o$)-1	ηred=ηsp/c
DMF	29.84	0	0
2	30.80	0.03217	0.01608
4	30.97	0.03786	0.00946
6	31	0.03887	0.00650
8	31.06	0.04088	0.00511
10	31.12	0.04289	0.00428
0.0065=int]η[	Mwt=2367.98		

Table 4. Data of C2 used to determine the intrinsic viscosity

C2 Compound concentration mg/ml	Time flow t/s	ηsp=(η/η$_o$=t/t$_o$)-1	ηred=ηsp/c
DMF	29.84	0	0
2	32.06	0.07439	0.03719
4	33.1	0.10924	0.02731
6	33.61	0.12634	0.021056
8	34.02	0.14008	0.01751
10	36.39	0.21950	0.02195
0.021=int]η[	Mwt=1239.765		

Table 5. Data of C3 used to determine the intrinsic viscosity

C3 Compound concentration mg/ml	Time flow t/s	ηsp=(η/η$_o$=t/t$_o$)-1	ηred=ηsp/c
DMF	29.84	0	0
2	30.81	0.03250	0.01625
4	30.90	0.03552	0.00888
6	31.10	0.04222	0.00703
8	31.40	0.05227	0.00653
10	31.65	0.06065	0.00606
0.007=int]η[	Mwt=2648.09		

Table 6 . Data of C4 used to determine the intrinsic viscosity

C4 Compound concentration mg/ml	Time flow t/s	ηsp=(η/η$_o$=t/t$_o$)-1	ηred=ηsp/c
DMF	29.84	0	0
2	30.87	0.03451	0.01725
4	31.20	0.04557	0.01139
6	31.23	0.04658	0.00776
8	31.67	0.06132	0.00766
10	32.62	0.09316	0.00931
0.0077=int]η[	Mwt=3039.17		

Table 7. Data of C5 used to determine the intrinsic viscosity.

C5 Compound concentration mg/ml	Time flow t/s	ηsp=(η/η$_o$=t/t$_o$)-1	ηred=ηsp/c
DMF	29.84	0	0
2	31.34	0.05026	0.02513
4	31.56	0.05764	0.01441
6	31.96	0.07104	0.01184
8	32.57	0.09148	0.01143
10	32.87	0.10154	0.01015
Int = 0.0118]η[	Mwt=5510.52		

Table 8. Data of C6 used to determine the intrinsic viscosity

C6 Compound concentration mg/ml	Time flow t/s	ηsp=(η/η$_o$=t/t$_o$)-1	ηred=ηsp/c
DMF	29.84	0	0
2	30.66	0.02747	0.01373
4	30.86	0.03418	0.00854
6	31	0.03887	0.00647
8	32.04	0.07372	0.00921
10	32.35	0.08411	0.00841
0.0064=int]η[	Mwt=2352.60		

The results presented in Table 9 and Fig. 8 demonstrate that all synthesized Schiff base compounds exhibit significant antibacterial activity against *Staphylococcus aureus*, while comparatively lower inhibition zones were observed against *Escherichia coli*. Most of the prepared compounds, tested in DMSO at a concentration of 0.1 mg/mL, showed stronger antibacterial activity toward Gram-positive bacteria than Gram-negative bacteria.

The enhanced activity against *S. aureus* can be attributed to structural differences in the bacterial cell wall. Gram-positive bacteria possess a relatively simpler peptidoglycan layer without an outer membrane, which facilitates the penetration of Schiff base molecules into the cell. In contrast, Gram-negative bacteria such as *E. coli* have an additional outer membrane composed of lipopolysaccharides that acts as a permeability barrier, limiting compound diffusion and thereby reducing antibacterial effectiveness.

These findings suggest that the synthesized Schiff base derivatives display selective antibacterial activity, with greater efficacy toward Gram-positive strains.

Table 9. Antibacterial Activity of Shiff Base [C1-C6]

Compounds	Inhibition zone for *Sample Staphylococcus* of polymer (mm)	Inhibition zone for *E.coli* of polymer (mm)
C1	15	8
C2	10	0
C3	10	0
C4	15	0
C5	16	8
C6	8	8

The synthesized compounds exhibit mild to moderate antibacterial activity, as evidenced by inhibition zones ranging from **8 to 16 mm**. The strongest activity was observed against *Staphylococcus aureus*, particularly for compounds **C1 (15 mm), C4 (15 mm), and C5 (16 mm)**. Although these values indicate appreciable antibacterial potential, they fall within the lower range reported for commonly used clinical antibiotics. For example, under standard disk-diffusion conditions, ampicillin typically produces inhibition zones of **18–30 mm** against *S. aureus*, gentamicin **15–22 mm**, and ciprofloxacin **20–34 mm**.

In contrast, antibacterial activity against *Escherichia coli* was comparatively weaker. Only **C1 and C5** demonstrated measurable inhibition zones (8 mm), whereas reference antibiotics such as ciprofloxacin and chloramphenicol generally produce inhibition zones of **20–30 mm** and **18–26 mm**, respectively, under similar experimental conditions.

These results suggest that while the synthesized Schiff base polymers exhibit notable activity against Gram-positive bacteria, their potency remains lower than that of established antibiotics, particularly against Gram-negative strains. The reduced effectiveness toward Gram-negative bacteria is consistent with the presence of an outer membrane that acts as a permeability barrier, limiting compound penetration and contributing to intrinsic resistance mechanisms [27–32].

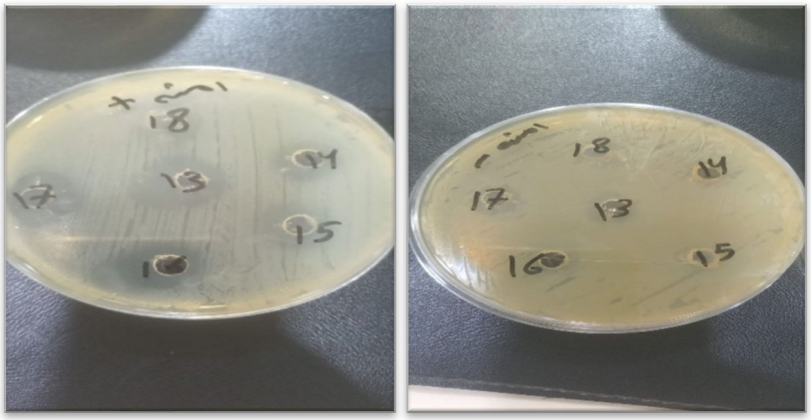

Fig. 8. Antibacterial activity *Gram-negative* bacteria and *Gram-positive* bacteria for [C1-C6]

Antioxidant Activity. The antioxidant activity of the synthesized compounds was evaluated using the DPPH (2,2-diphenyl-1-picrylhydrazyl) radical scavenging assay. A DPPH solution was prepared by dissolving 0.002 g of DPPH in 100 mL of ethanol and stirring for 5 minutes using a magnetic stirrer. Ascorbic acid, used as the reference standard, was dissolved in a 1:1 mixture of ethanol and deionized water to obtain concentrations of 250, 125, 62.5, and 31.25 µg/mL, with continuous stirring for 5 minutes to ensure complete dissolution.

For the assay, 1 mL of DPPH solution was mixed with 1 mL of each test sample (C1–C6) at the same concentrations (250, 125, 62.5, and 31.25 µg/mL). The reaction mixtures were incubated in

the dark at room temperature for 30 minutes to prevent photo-degradation. After incubation, the optical density (OD) of each solution was measured spectrophotometrically.

The antioxidant activity results (Table 9) indicate that most of the synthesized compounds exhibited moderate to strong radical scavenging activity compared with the reference standard (ascorbic acid). Among the tested compounds, C3 demonstrated the highest antioxidant activity, whereas C6 showed the lowest activity. Based on the comparative radical scavenging performance, the antioxidant activity follows the order:

C3 > C4 > C2 > C1 > ascorbic acid > C5 > C6

Table 10. Show the Activity of Antioxidant for C1-C6

Conc. µg/ml)(	**Activity (%)**						
	C1	**C2**	**C3**	**C4**	**C5**	**C6**	A.C.
31.25	60.86	69.16	71.78	51.21	5.56	4.28	65.84
62.50	74.65	79.76	88.12	78.29	48.34	8.17	70.88
100	86.46	86.85	89.34	88.70	72.86	45.85	77.46
250	90.74	91.32	92.78	91.95	82.70	70.50	84.48

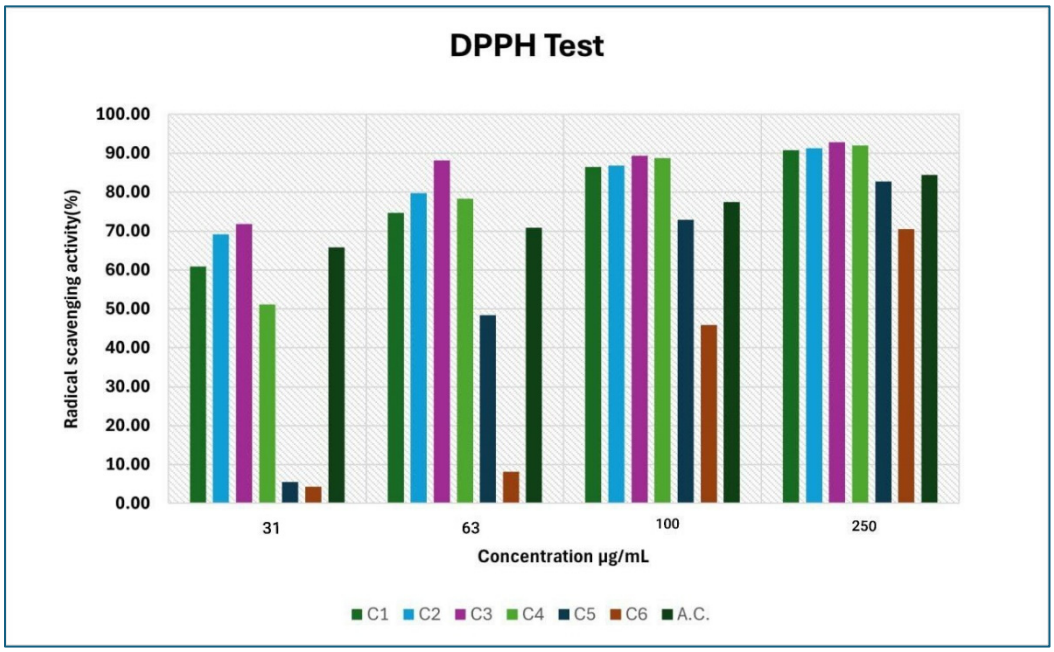

Fig. 9. Graph showing DPPH scavenging activities of Schiff base (C1-C6).

Conclusion

A new series of Schiff-base polymers was obtained by reacting polyacrylic acid with a bridging spacer followed by condensation with aldehydes. Structural confirmation was achieved through infrared and nuclear magnetic resonance spectroscopy. Their physical behavior was evaluated through solubility tests in both polar and nonpolar solvents, showing partial solubility in most media and complete dissolution in DMF, DMSO, and chloroform. Viscosity studies were then performed in DMF at 37 °C using an Ostwald viscometer (0.49 mm capillary) across a concentration range of 10–2%.

Biological assays demonstrated that the synthesized Schiff-base materials display greater inhibition toward Gram-positive bacteria than Gram-negative strains. Antioxidant screening further revealed variation among the compounds, with C3 exhibiting the highest radical-scavenging activity. These combined results highlight the potential multifunctional behavior of the prepared polymers.

References

1. Vashist A., Vashist A., Gupta Y.K., Ahmad S. Recent advances in hydrogel based drug delivery systems for the human body. *Journal of Materials Chemistry B*, 2014, **Vol. 2(2)**, p. 147-66. DOI: 10.1039/C3TB21016B
2. Matricardi P., Di Meo C., Coviello T., Hennink W.E., Alhaique F. Interpenetrating polymer networks polysaccharide hydrogels for drug delivery and tissue engineering. *Advanced drug delivery reviews*, 2013, **Vol. 65(9)**, p. 1172-1187. DOI: 10.1016/j.addr.2013.04.002
3. Costa D., Valente A.J., Miguel M.G., Queiroz J. Gel network photodisruption: a new strategy for the codelivery of plasmid DNA and drugs. *Langmuir,* 2011, **Vol. 27(22)**, p. 13780-13789. DOI: 10.1021/la2026285
4. Qiu Y., Park K. Environment-sensitive hydrogels for drug delivery. *Advanced drug delivery reviews*, 2001, **Vol. 53(3)**, p. 321-339. DOI: 10.1016/S0169-409X(01)00203-4
5. Pavlinec J., Novák I., Rychlý J., Kleinová A., Nógellová Z., Preťo J., Vanko V., Žigo O., Chodák I. Hot melt adhesives prepared by grafting of acrylic and crotonic acids onto metallocene ethylene–octene copolymers. *Journal of Plastic Film & Sheeting*, 2019, **Vol. 35(3)**, p. 239-259. DOI: 10.1177/8756087918820904
6. Dashtizadeh A., Abdouss M., Khorassani M., Mahdavi H. Preparation of silica-filled water-based acrylic nanocomposite paints with improved scratch resistance. *Journal of Plastic Film & Sheeting*, 2012, **Vol. 28(2)**, p. 120-135. DOI: 10.1177/8756087911421702
7. Savaskan Y.S., Yildirim N., Misir M., Misirlioglu Y., Celik E. Synthesis, characterization of a new polyacrylic acid superabsorbent, some heavy metal ion sorption, the adsorption isotherms, and quantum chemical investigation. *Materials*, 2020, **Vol. 13(19)**, 4390. DOI: 10.3390/ma13194390
8. Yee S.Y. Medicinal properties of bioactive compounds and antioxidant activity in Durio zibethinus. *Malays. J. Sustain. Agric.,* 2021, **Vol. 5**, p. 82-89. DOI: 10.26480/mjsa.02.2021.82.89
9. Vigato P.A., Tamburini S. The challenge of cyclic and acyclic Schiff bases and related derivatives. *Coordination Chemistry Reviews*, 2004, **Vol. 248(17-20)**, p. 1717-2128. DOI: 10.1016/j.cct.2003.09.003
10. Kuddushi M.M., Malek M.A., Patidar V.L., Patel M.S., Patel R.K., Dave R.H. Synthesis and characterization of Schiff base aniline with 5-bromo-2-hydroxyl benzaldehyde and their metal complexes. *Int. J. Recent Sci. Res.*, 2018, **Vol. 9(4)**, p. 26026-26030. DOI: 10.24327/ijrsr.2018.0904.1977
11. Supuran C.T., Barboiu M., Luca C., Pop E., Brewster M.E., Dinculescu A. Carbonic anhydrase activators. Part 14. Syntheses of mono and bis pyridinium salt derivatives of 2-amino-5-(2-aminoethyl)-and 2-amino-5-(3-aminopropyl)-1, 3, 4-thiadiazole and their interaction with isozyme II. *European journal of medicinal chemistry*, 1996. **Vol. 31(7-8)**, p. 597-606. DOI: 10.1016/0223-5234(96)89555-9
12. Abdul-Majid Q. *Some Aspects of Carbon-Nitrogen Double Bond Photochemistry*. The University of Manchester (United Kingdom). 1982.
13. Venugopala K.N., Jayashree B.S. Synthesis of carboxamides of 2′-amino-4′-(6-bromo-3-coumarinyl) thiazole as analgesic and antiinflammatory agents. *Indian Journal of Heterocyclic Chemistry*, 2003, **Vol. 12(4)**, p. 307-310.
14. Vashi K., Naik H.B. Synthesis of novel Schiff base and azetidinone derivatives and their antibacterial activity. *Journal of Chemistry*, 2004, **Vol. 1(5)**, p. 272-275. DOI: 10.1155/2004/158924
15. Dhar D.N., Taploo C.L. Schiff bases and their applications. *J. Sci. Ind. Res.,* 1982, **Vol. 41(8),** p. 501-506.
16. Li S., Chen S., Lei S., Ma H., Yu R., Liu D. Investigation on some Schiff bases as HCl corrosioninhibitors for copper. *Corrosion Science*, 1999, **Vol. 41(7)**, p. 1273-1287. DOI: 10.1016/S0010-938X(98)00183-8
17. Chohan Z.H., Praveen M., Ghaffar A. Structural and Biological Behaviour of Co (II), Cu (II) and Ni (II) Metal Complexes of Some Amino Acid Derived Schiff-Bases. *Metal-Based Drugs*, 1997, **Vol. 4(5)**, p. 267-272. DOI: 10.1155/MBD.1997.267

18. Ershad S., Sagathforoush L.A., Karim-nezhad G., Kangari S. Electrochemical behavior of N_2SO Schiff-base Co (II) complexes in non-aqueous media at the surface of solid electrodes. *International Journal of Electrochemical Science*, 2009, **Vol. 4(6)**, p. 846-854. DOI: 10.1016/S1452-3981(23)15188-1
19. Bhattacharya A., Purohit V.C., Rinaldi F. Environmentally friendly solvent-free processes: novel dual catalyst system in Henry reaction. *Organic process research & development*, 2003, **Vol. 7(3)**, p. 254-258. DOI: 10.1021/op020222c
20. Gopalakrishnan M., Sureshkumar P., Kanagarajan V., Thanusu J. New environmentally-friendly solvent-free synthesis of imines using calcium oxide under microwave irradiation. *Research on Chemical Intermediates*, 2007, **Vol. 33(6)**, p. 541-548. DOI: 10.1163/156856707782565822
21. Das S., Das V.K., Saikia L., Thakur A.J. Environment-friendly and solvent-free synthesis of symmetrical bis-imines under microwave irradiation. *Green Chemistry Letters and Reviews,* 2012, **Vol. 5(3)**, p. 457-474. DOI: 10.1080/17518253.2012.667443
22. Taslı P.T., Bayrakdar A., Karakus O.O., Kart H.H., Koc Y. Synthesis and characterization of three novel Schiff base compounds: Experimental and theoretical study. *Optics and Spectroscopy*, 2015, **Vol. 119(3)**, p. 467-484. DOI: 10.1134/S0030400X15090222
23. Yıldız E., Köse M., Tümer M., Purtaş S., Tümer F. Thiophene based imine compounds: Structural characterization, electrochemical, photophysical and thermal properties. *Journal of Molecular Structure*, 2017, **Vol. 1150**, p. 55-60. DOI: 10.1016/j.molstruc.2017.08.042
24. Aytac S., Gundogdu O., Bingol Z., Gulcin İ. Synthesis of Schiff bases containing phenol rings and investigation of their antioxidant capacity, anticholinesterase, butyrylcholinesterase, and carbonic anhydrase inhibition properties. *Pharmaceutics*, 2023, **Vol. 15(3)**, 779. DOI: 10.3390/pharmaceutics15030779
25. Fadel F.J., Kareem M.M., Mohammed F.H. New glycogen derivatives as an advantageous polymers carrier in bacteria theranostics. *Chemical Problems*, 2025, **Vol. 23(2)**, p. 166-77. DOI: 10.32737/2221-8688-2025-2-166-177
26. Kim S.J., Lee C.K., Lee Y.M., Kim I.Y., Kim S.I. Electrical/pH-sensitive swelling behavior of polyelectrolyte hydrogels prepared with hyaluronic acid–poly (vinyl alcohol) interpenetrating polymer networks. *Reactive and Functional Polymers*, 2003, **Vol. 55(3)**, p. 291-298. DOI: 10.1016/S1381-5148(03)00019-1
27. Mohammed I.A., Kareem M.M. Synthesis, characterization and study of some of new mefenamic acid derivatives as cytotoxic agents. *Int. Journal of Physics: Conference Series*, 2020, **Vol. 1664(1)**, 012081. DOI: 10.1088/1742-6596/1664/1/012081
28. Fu X., Liao Y., Glein C.R., Jamison M., Hayes K., Zaporski J., Yang Z. Direct synthesis of amides from amines and carboxylic acids under hydrothermal conditions. *ACS Earth and Space Chemistry*, 2020, **Vol. 4(5)**, p. 722-729. DOI: 10.1021/acsearthspacechem.0c00009
29. Singh K., Barwa M.S., Tyagi P. Synthesis, characterization and biological studies of Co (II), Ni (II), Cu (II) and Zn (II) complexes with bidentate Schiff bases derived by heterocyclic ketone. *European Journal of Medicinal Chemistry*, 2006, **Vol. 41(1)**, p. 147-153. DOI: 10.1016/j.ejmech.2005.06.006
30. Ahmed S.Y., Abdul-Rida N.A. Synthesis and biological activity evaluation for ester derivatives from some nsaids drugs. *Chemical Problems*, 2026, **Vol. 24(1)**, p. 55-61. DOI: 10.65382/2221-8688-2026-1-55-61
31. Duha A.M., Mohanad M.K., Israa N.W. New n-substituted itaconimide polymers: synthesis, characterization and biological activity. *Eurasian Chemical Communications*, 2023, **Vol. 5(9)**, p. 866-884. DOI: 10.22034/ecc.2023.397194.1643
32. Kareem M.M., Nour A., Saadon A., Nagham M.A. Synthesis, Characterization and Biological activity study for new hybrid polymers by grafting 1, 3, 4-triazole and 1, 2, 4-oxadiazle moieties onto polyvinyl chloride. *Egypt J Chem*. 2021, **Vol. 64(3),** p. 1273-1284. DOI: 10.21608/EJCHEM.2021.27879.2584